Experimental Neurology 311 (2019) 213–224

Contents lists available at ScienceDirect

Experimental Neurology

journal homepage: www.elsevier.com/locate/yexnr

Research Paper

Long-term social isolation inhibits autophagy activation, induces postsynaptic dysfunctions and impairs spatial memory

Bin Wang[a,1], Qiong Wu[a,1], Lei Lei[b,1], Hailun Sun[a], Ntim Michael[a], Xuan Zhang[b], Ying Wang[d,c], Yue Zhang[a], Biying Ge[b], Xuefei Wu[a], Yue Wang[d], Yi Xin[c,***], Jie Zhao[b,**], Shao Li[a,*]

[a] Liaoning Provincial Key Laboratory of Cerebral Diseases, Department of Physiology, Dalian Medical University, Dalian, Liaoning, China
[b] Technology Centre of Target-based Nature Products for Prevention and Treatment of Ageing-related Neurodegeneration, Dalian Medical University, Dalian, Liaoning, China
[c] Department of Biochemistry and Molecular Biology, Dalian Medical University, Dalian, Liaoning, China
[d] Department of Cardiology, Institute of Heart and Vessel Diseases of Dalian Medical University, the Second Affiliated Hospital of Dalian Medical University, Dalian, Liaoning, China

ARTICLE INFO

Keywords:
Social isolation
Cognition
Long-term potentiation
NMDARs
AMPARs
PSD-95
Autophagy

ABSTRACT

Social isolation in adolescence leads to lasting deficits in hippocampal-dependent tasks. The reported effects of isolation on learning and memory in the Morris water maze and synaptic-related proteins have been inconsistent. Moreover, the autophagy level and its effect on cognition in the isolation model are also not clear. In the present study, we did an extended isolation period up to six months to establish a stable and appropriate isolation model to investigate the cognitive changes associated with it. The mTOR inhibitor rapamycin was systemically administered to mice to determine the roles of autophagy activation on cognitive changes. We discovered that long-term post-weaning social isolation (L-PWSI) produced marked deficits in spatial learning and memory and inhibited CA1 long-term potentiation (LTP), but paired-pulse facilitation (PPF) and input/output (I/O) curve were unaffected. The results further showed that the L-PWSI significantly decreased the protein expression levels of PSD-95, GluA1, NR1 and NR2B in the hippocampus, and no significant changes in the extracellular release of glutamate and the protein expression levels of synaptophysin, synapsin I, GAP-43, NR2A and $GABA_A$. Moreover, we found that L-PWSI increased the protein expression of p-AKT/AKT, p-mTOR/mTOR and p62, whereas the protein levels of LC3B and Beclin1 were decreased indicating an inhibition in autophagy activity. Intraperitoneal injection of rapamycin significantly potentiated fEPSP slope and cognition-related proteins expression in the L-PWSI mice. These results therefore suggest that L-PWSI induces postsynaptic dysfunction by disrupting the interaction between AMPAR, NMDAR and PSD-95, and inhibit the autophagy activity which led to impaired spatial memory and cognitive function.

1. Introduction

Social isolation (SI) is an objective reflection of reduced social network size or lack of social contact, rearing of rodents with SI stress during the early weaning periods induce numerous behavioral, morphological and functional abnormalities of the central nervous system (Khodaie et al., 2015; Okada et al., 2014b; Murai et al., 2007). This could damage the development and maturation of the brain, which will ultimately result in cognitive impairment (Yusufishaq and Rosenkranz, 2013). However, related researches have also reported that social isolation (SI) induced poorer performance (Lu et al., 2003; Hellemans et al., 2004), better performance (Wongwitdecha and Marsden, 1996), or had no effect (Riley et al., 2016) on spatial cognition. These reports on the effects of isolation on spatial cognition are inconsistent. Meanwhile, there have not been a definite report on the effects of SI with regards to the expression of proteins involved (Levine et al., 2007; Zhao

* Corresponding author.
** Correspondence to: Jie Zhao, Technology Centre of Target-based Nature Products for Prevention and Treatment of Ageing-related Neurodegeneration, Dalian Medical University, Dalian, Liaoning, China
*** Correspondence to: Yi Xin, Department of Biochemistry and Molecular Biology, Dalian Medical University, Dalian, Liaoning, China
E-mail addresses: wb101900@163.com, 642698048@qq.com (B. Wang), jimxin@hotmail.com (Y. Xin), zhaoj@dmu.edu.cn (J. Zhao), lishao89@dmu.edu.cn (S. Li).
[1] These authors contributed equally to this work.

https://doi.org/10.1016/j.expneurol.2018.09.009
Received 28 March 2018; Received in revised form 14 August 2018; Accepted 12 September 2018
Available online 13 September 2018

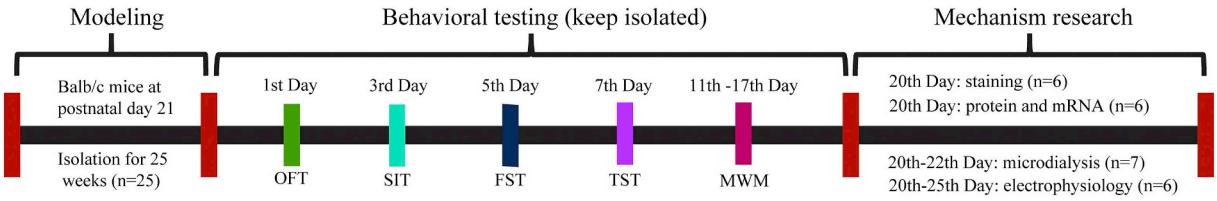

Fig. 1. Experimental timeline. The L-PWSI mice were individually housed from postnatal day 21 for 25 weeks, and the control mice were group housing. After the modeling, the animals underwent weeks of behavioral testing (the L-PWSI mice were still isolation). The mice were allowed to rest every other day during the behaviour testing. At the end of experiment animals were sacrificed for microdialysis, electrophysiology, staining and samples collected for western-blot and RT-PCR.

et al., 2009), and this has left a huge gap in the detailed mechanism of these effects.

The isolation period of SI model usually ranges from 2, 4, 6 to 8 weeks from the time of weaning at 21 days of age (Chen et al., 2017a; Lu et al., 2003; Wongwitdecha and Marsden, 1996). All of these staged at a phase of dynamic cognitive development that occurs during childhood through to adolescence in the human. This represents a transitional period and enhanced activation of brain circuitry that occur with age (Paus et al., 2008; Brenhouse and Andersen, 2011). In addition, during the "emerging adulthood" stage, which ranges from age 18 to 29 years of age in humans, the brain has also not achieved maturity but is generally becoming more stable (Arnett, 2000; Negru-Subtirica et al., 2016). The dynamic process of brain development may perturb or hide the effects of short-term isolation stress on cognitive function and proteins expression. To detect the effect of SI more convincingly, we modeled the long-term post-weaning social isolation (L-PWSI) in which the period of the chronic social isolation model was done up to 6 months of social isolation.

Together with long-term depression (LTD), metaplasticity, homeostatic plasticity and spike-timing-dependent plasticity (STDP), long-term potentiation (LTP) remains the best-known and most intensively studied form of activity-dependent synaptic plasticity. The long-term studies suggest that the mechanisms involved in the generation of LTP are the synaptic basis of memory (Bliss and Collingridge, 1993; Bliss et al., 2014). The release of glutamate can bind to both postsynaptic α-amino-3-hydroxy-5-methyl-4-isoxazole propionic acid receptor (AMPAR) and *N*-methyl-D-aspartate receptors (NMDARs). NMDARs are well known for their role in the induction of LTP (Wang and Peng, 2016; Volianskis et al., 2015). Postsynaptic density-95 (PSD-95) is a prominent postsynaptic membrane protein involved in synaptic plasticity (Liu et al., 2008; Wang et al., 2016). Synaptophysin and synapsin I are abundant synaptic vesicle proteins which provide the anatomical basis of quantal release of glutamate (Greengard et al., 1993; Tarsa and Goda, 2002). Compelling evidence has supported the role of synaptophysin, synapsin I, GAP43 and PSD95 in the stimulation of synapse formation and reconstruction (Donovan et al., 2002; Kwon and Chapman, 2011). Thus, besides the recording of the signal of field excitatory post-synaptic potentials (fEPSP), we measured the expression levels of cognition- and synaptic-related proteins as well as the extracellular level of glutamate which regulate various memory-connected activities using microdialysis.

Autophagy is an intracellular protein degradation system which plays a vital role in the interaction with apoptosis by controlling the balance between protein synthesis and degradation (Hsieh et al., 2011; Yen et al., 2013). It is well known that constitutive autophagy is responsible for neuronal survival (Poels et al., 2012) and protects neurons from nutritional starvation (Kaushik et al., 2011). Increasing evidence has revealed that the dysfunction of autophagy causes many neurodegenerative diseases and behavioral deficits (Hara et al., 2006; Komatsu et al., 2006). There are several key molecular components which participate in the initiation, progression and completion of autophagy, such as the mammalian target of rapamycin (mTOR), which inhibits autophagy, and Beclin1 as well as light chain (LC) 3, which promote it (Cordaro et al., 2016). In addition, P62, as an autophagy substrate, is degraded during autophagy activation (Lau et al., 2013). Our research also focused on these autophagy-related proteins expression and the results bring to bare, the cognitive changes induced by the L-PWSI as well as the role autophagy plays in this cognitive change.

2. Materials and methods

2.1. Animals and behaviors detection

Male Balb/c mice were purchased from the Laboratory Center of Dalian Medical University. The mice were assigned to group housing versus isolation housing with free access to food and water. The animals were housed in polypropylene cages with woodchip bedding, and the housing rooms were set to a 12-h day/night cycle at 21 ± 1 °C and 55 ± 5% humidity. See Supplemental Methods for ethics protocols. For the L-PWSI model, the mice were separated and individually housed in cages from the first weaning day, which is postnatal day 21, and the isolation period lasted for approximately 25 weeks until the mice were 28 weeks of age. The isolated mice only had auditory and olfactory contact with other conspecifics without any form of physical interaction or visual contact with the other conspecifics. The open-field test (OFT), social interaction test (SIT), forced swimming test (FST) and tail suspension test (TST) were performed after the modeling (Rodríguez-Arias et al., 2015; Kumari et al., 2016; Ma et al., 2017). The time-table for behavioral testing as well as when brains were collected for electrophysiology/molecular work is shown in Fig. 1.

Open-field test: The OFT is commonly used to assess basic locomotor activity as well as anxiety-like behavior (Zaidan and Gaisler-Salomon, 2015). The test was performed in a white plexiglass arena (50 cm × 50 cm × 40 cm) for 5 min. The total distance travelled (cm) and mobile cumulative duration (s), velocity (cm/s), the frequency and time (s) spent in the center of the arena were assessed.

Social interaction test: The SIT test included the social mice and experimental mice. Three neighbouring rooms of same size (40 cm × 40 cm × 20 cm) were used with an empty room of the behavior observation box in the middle, using opaque plexiglass panels isolated the bilateral room. Before the test, the experimental mouse was placed into the middle room for 5 mins, and the social mouse was randomly placed into one side room. Then, the panel was removed and the interaction behaviors between the experimental mouse and the social mouse were videotaped for subsequent analysis. The time of attack was recorded within 5 mins interaction.

Forced Swim Test: To assess depression-like behavior, mice were individually placed polymethylpentene cylinder (diameter: 12 cm, height: 27 cm) containing 25 ± 1 °C water of depth 14 cm for a total duration of 6 mins and the swimming session was videotaped using a digital video camera for subsequent analysis. Immobility time (inactive cumulative duration) was assessed during the last 5 mins of the 6-min trial as previously described (O'Keefe et al., 2014).

Tail suspension test: The TST was also performed for the detection of depressive behaviors (Cryan et al., 2015). Mice were suspended horizontally by the tail for 6 mins, and the moving session was videotaped for subsequent analysis. Immobility time (inactive cumulative duration) was assessed during the last 5 min of the 6-min trial.

2.2. Morris water maze

The MWM test was performed as described by Morris (Morris, 1984; Chen et al., 2013), and the animals were handled by the experimenter in the water maze room for a few minutes. The acquisition phase consisted of 5 consecutive trial days (3 trials per day, each trial 90 s). A different starting quadrant was used for each trial. Once the mouse found the platform, it was allowed to remain there for 10 s. If the mouse failed to find the platform in 90 s, then the mouse was gently guided to the platform and allowed to remain there for 10 s. The location of release was counterbalanced both within and between the groups. The escape latencies (time spent swimming from the start point to the platform) and the mean swim speed before reaching the platform were recorded as an index of spatial learning. The escape latency of the mice on the first training day was normalized to 1.0, and the relative escape latencies for the following training days were calculated relative to those of the first day (escape latency in the following day/escape latency in the first day). The memory consolidation test was administered 24 h later using the same setup with the exception of the removal of escape platform. Each mouse was allowed to swim freely for 90 s in the pool. The activities measured included swimming speed and the numbers of platform-site crossovers. The swimming path of the mice was recorded using a camera installed 2.0 m above the centre of the pool and analyzed using a computerized video tracking system (Ethovision 2.0, Noldus, Wagenigen, Netherlands).

2.3. Primary and secondary antibodies

The following antibodies were used: anti-β-actin (ab6276, Abcam, USA), anti-α-Amino-3-hydroxy-5-methyl-4-isoxazolepropionic acid (AMPA) glutamate receptor 1 (GluA1, ab31232, Abcam), anti-PSD-95 (ab2723, Abcam), anti-NR1 (556,308, BD Pharmingen), anti-synaptophysin (MAB5258, Millipore), anti-synapsin I (ab64581, Abcam), anti-NR2B (ab93610, Abcam) and anti-NR2A (ab84181, Abcam), anti-p62/SQSTM1 (P0067, Sigma-aldrich), anti-Beclin 1 (ab62557, Abcam), anti-LC3B (#3868, Cell Signaling), anti-Phospho-mTOR(Ser2448) (#5536, Cell Signaling), mTOR (#2983, Cell Signaling), anti-GAP43 (AB5220, Millipore), anti-Akt (#2920, Cell Signaling), anti-Phospho-Akt (#4060, Cell Signaling), horseradish peroxidase-labelled secondary antibodies (ZSJQ-BIO Company, Beijing, China).

2.4. Electrophysiology and recording

The electrophysiological recording experiment was carried out according to a previously described method (Zhang et al., 2014; Lin et al., 2017a). Transverse hippocampal slices (400 μm) were prepared from dorsal hippocampus and stored in artificial cerebral spinal fluid (saturated in 95% O2 and 5% CO2, pH 7.4) for at least 1 h before being removed to a submersion-recording chamber, which was continually perfused with oxygenated cerebrospinal fluid at a rate of 1–2 mL per minute. Field excitatory postsynaptic potential (fEPSP) was evoked in the stratum radiatum of the hippocampal CA1 region by means of a glass microelectrode (Frederick Haer Co) filled with 3 M NaCl. The Schaffer collateral pathway was stimulated with concentric bipolar electrodes positioned in the stratum radiatum. The stimulation pulse (0.2 ms duration, 0.033 Hz) selected for baseline measurements was adjusted to yield ~40% of its maximal slope. After baseline responses had stabilized for 30 min, long-term potentiation (LTP) was induced using high-frequency stimulation (four 100 Hz and 1 s trains delivered 20 s apart). The electrophysiological data were acquired with an Axon multiclamp 700 B amplifier, filtered at 0.1–5 KHz, and digitized at 10 KHz, and the slope, peak amplitude, and initial area of fEPSP were measured and analyzed offline using pClamp10.3 software (Molecular Devices Corp, USA).

Input/output (I/O) curves are normally generated to assess basal synaptic transmission, the average of three pulses delivered at 0.033 Hz, 0.2 ms duration at each intensity in the range of 0.05–1 mA in steps of 0.05 mA. Paired-pulse facilitation (PPF) is a form of short-term synaptic plasticity, we applied paired-pulse stimulation (The stimulation was adjusted to yield ~40% of its maximal slope) at inter-stimulus intervals of 0, 50, 100, 150, 200 and 250 ms. The paired-pulse ratio was calculated as the amplitude of the fEPSP elicited by the second pulse divided by the amplitude elicited by the first.

2.5. In vivo microdialysis

In vivo microdialysis was carried out according to our previously described method (Wang et al., 2017). The mice were anaesthetized with pentobarbital (50 mg/kg, i.p.) and were fixed in a stereotactic frame (SR-5 M, Narishige, Tokyo, Japan). The intracerebral guide cannula (MBR-5, BASI, West Lafayette, IN 47906 USA) was implanted 1 mm above the hippocampus (A: −2.06 anterolateral, L: ± 1.1 mm mediolateral from the bregma; V: −2.25 mm dorsoventral to the dura) and was secured onto the skull with stainless steel screws and dental acrylic cement. After 24 h, a microdialysis probe (MBR-1-5, 1 mm membrane length, BASI) was embedded into the guide cannula, and the ACSF was continuously perfused into the hypothalamus through the probe. During the microdialysis experiments, dialysates were collected in 1-h increments at a velocity of 1 μL/min, and then 50 μL aliquots were used to measure glutamate levels with an ELISA kit (SU-B20731, Crodis biotech, Quanzhou, China).

2.6. Western blot

The western-blot experiment was carried out according to a previously described method (Wang et al., 2017). The protein from the hippocampus was extracted by using an extraction kit (Keygen Biotech, China), and the protein content was measured by a BCA protein assay (Keygen Biotech, China). The proteins (20 μg) for each sample were loaded into a 10% SDS PAGE gel for electrophoresis. Then, the protein components were transferred to polyvinylidene difluoride (PVDF) membranes, and then blocked with 5% BSA in TBST (TBS + 0.1% Tween-20) for 1 h, and then immunoblotted overnight at 4 °C with the primary antibodies. Subsequently, the membranes were washed three times in TBST and incubated with a horseradish peroxidase-labelled secondary antibody (anti-rabbit or anti-mouse, 1:5000; ZSJQ-BIO Company, Beijing, China) for 1 h at room temperature. The infrared band signals were detected using BIO-RAD (Hercules, CA, USA) gel analysis software. The blots were then washed with TBST, blocked for 1 h and incubated with the primary antibody for β-actin for the loading control. The densitometric analysis of immunoreactivity was conducted using the NIH Image J software and normalized to the immunoreactivity of the group-housed animals.

2.7. Reverse transcriptase-PCR (RT-PCR)

Total RNA was extracted from hippocampal tissue using TRI reagent (Sigma-Aldrich, MO, USA), cDNA was synthesized by a TransScript One-Step gDNA Removal and cDNA Synthesis Super Mix (TransGen Biotech, Beijing, China). The cDNA was amplified with primer and performed with reagents, the primers for GluA1, NR2B, NR1, PSD-95 and the housekeeping gene GAPDH (Life Technologies, Thermo Fisher Scientific-CN, Shanghai, China) are listed in Table 1. The amplified samples were further run on a 2% agarose gel followed by a UV transilluminator and photography for visualization. The values obtained for the target gene expression were normalized to GAPDH and quantified relative to the expression in control samples. The products were analyzed by densitometry using the NIH Image J and Quantity One software (BioRad, Hercules, CA, USA).

Table 1
Primer sequences for RT-PCR analysis.

Target mRNA sequences	Primer sequence
GluA1	5′-GAGCAACGAAAGCCCTGTGA-3′ 5′-CCCTTGGGTGTCGCAATG-3′
NR2B	5′-GCCATGAACGAGACTGACCC-3′ 5′-GCTTCCTGGTCCGTGTCATC-3′
NR1	5′-AGTGGAACGGAATGATGGGAG-3′ 5′-CCGAACCCATGTCTTATCCAG-3′
PSD-95	5′-TGAGATCAGTCATAGCAGCTACT-3′ 5′-CTTCCTCCCCTAGCAGGTCC-3′
GAPDH	5′-CACTGGCATGGCCTTCCGT-3′ 5′-CTTACTCCTTGGAGGCCAT-3′

2.8. Immunohistochemistry and immunofluorescence staining

The mice were anaesthetized with pentobarbital (50 mg/kg, i.p.) and then perfused with 0.1% phosphate buffer (PB) followed by 4% paraformaldehyde (PFA) dissolved in 0.1% PB. The brains were removed and left in 4% PFA at 4 °C for 24 h then transferred to 30% sucrose dissolved in 0.1% PB. Following saturation of the brains in sucrose, serial 15 μm coronal sections were made with a cryostat (Leica CM 3050 S, Leica Microsystems AG, Wetzlar, Germany) after OCT embedding. The slices that contain ventral hippocampus were used for the staining.

For the immunohistochemistry staining procedure, the slices were thoroughly rinsed in 0.01 M PBS then quenched in 3% H_2O_2 in 0.01 M PBS for 15 min. They were subsequently thoroughly rinsed again then pre-incubated for 1 h in 2% bull serum albumin (BSA) and 0.3% Triton X-100 in 0.01 M PBS at room temperature and then incubated at 4 °C with one of the following primary antibodies: mouse anti-PSD95, rabbit anti-GluA1 and mouse anti-NR1 in 0.01 M PBS containing 2% BSA and 0.3% Triton X-100 overnight. After incubation with a biotinylated goat anti-rabbit or anti-mouse IgG secondary antibody (1:200; Vector Laboratories, Burlingame, CA, USA) for 2 h, the bound antibodies were visualized using an avidin–biotin–peroxidase complex system (Vectastain ABC Elite Kit, Vector Laboratories, Burlingame, CA, USA) and the stained with diaminobenzidine (DAB; Vectro Laboratories) as a chromogen. The slides were visualized with a microscopy and digitally photographed (Pannoramic Digital Slide Scanners, 3DHISTECH, Budapest, Hungary). The analysis of mean integrated optical density (MIOD) for NR1 and PSD-95 were performed using Image J software of National Institutes of Health as described previously (Jung et al., 2010; Avdalyan et al., 2015).

For the immunofluorescence staining procedure, the slices were permeabilized with 0.3% Triton X-100 in 0.01 M PBS for 15 min and then pre-incubated for 1 h in 5% bull serum albumin (BSA), followed by incubation with primary antibodies: mouse anti-PSD-95 overnight at 4 °C. After incubation for 2 h with anti-mouse Alexa Fluor 594 (1:200; Beyotime Institute of Biotechnology, Shanghai, China), the sections were washed in PBS for 3 × 5 min, and then incubation with 4′,6-diamidino-2-phenylindole for 10 min (DAPI, 1:10; Beyotime Institute of Biotechnology, Shanghai, China) and then coverslipped with DIwater/glycerol. Images were acquired from a microscope (Leica, Wetzlar, Germany) and digitally photographed. Three mice per group were analyzed, and serials slides of each mouse were collected. The analysis was performed in the slides from the same regions of each group of the mice. Quantitative analysis of mean fluorescent intensity (MFI) were performed using Image J software of National Institutes of Health as described in Ding et al. (Ding et al., 2008, Tao et al., 2016).

2.9. Statistical analysis

The data were analyzed using GraphPad Prism (GraphPad Software Inc.) and SPSS 21.0, expressed as the mean ± SEM. Student 2-tailed unpaired *t*-test was used to analyse the variance between the L-PWSI group and the control group, two way ANOVA was used to evaluate the effects of rapamycin between groups (Fig. 7G.I). The data summarized in Figs. 3A. B. E, 4E. F and 5A were assessed by repeated-measures ANOVA. $p < 0.05$ was considered statistically significant.

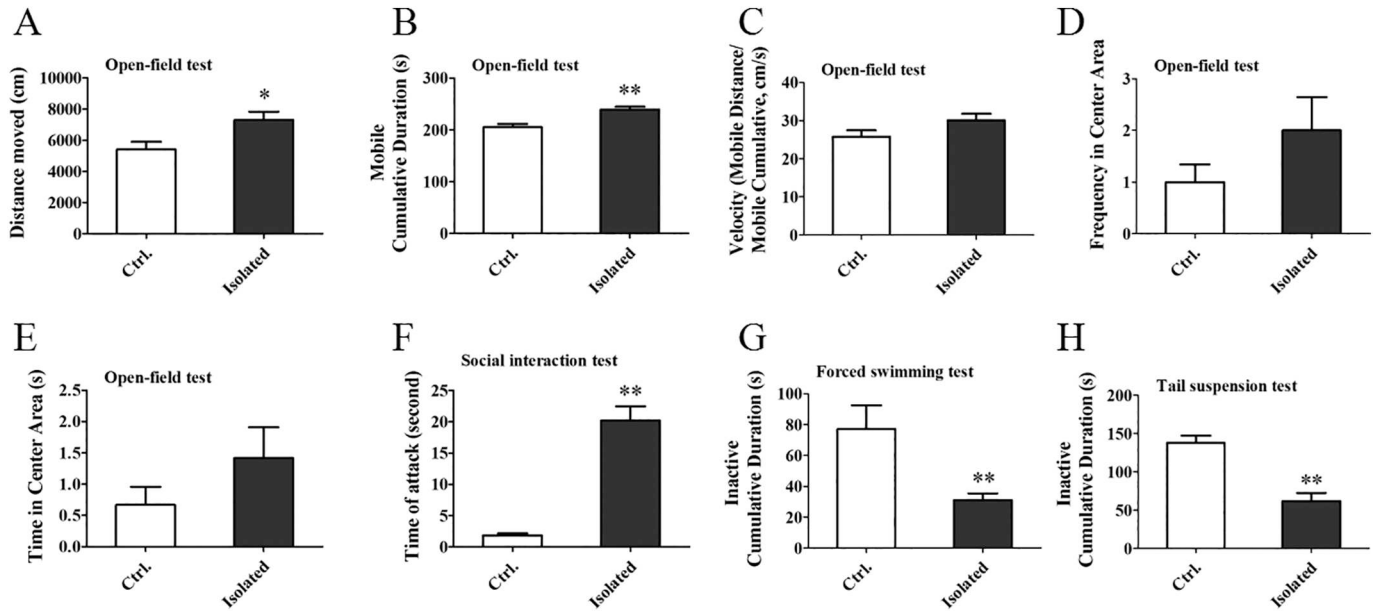

Fig. 2. The results of open-field test, social interaction test, forced swimming test and tail suspension test in the L-PWSI and control groups of mice. Means of distance moved (A), mobile cumulative duration (B), mobile velocity (C) and the number of crosses and time in the center zone (D.E) exhibited by the control and isolated group during the open-field test. (F) Means of accumulated times (in seconds) spent in attack exhibited by the control and isolated group during the social interaction test. (G.H) Means of inactive cumulative durations exhibited by the control and isolated group during the forced swimming test and tail suspension test. Data are presented as the mean ± SEM from 22 mice in each group. * represents $p < 0.05$; ** represents $p < 0.01$.

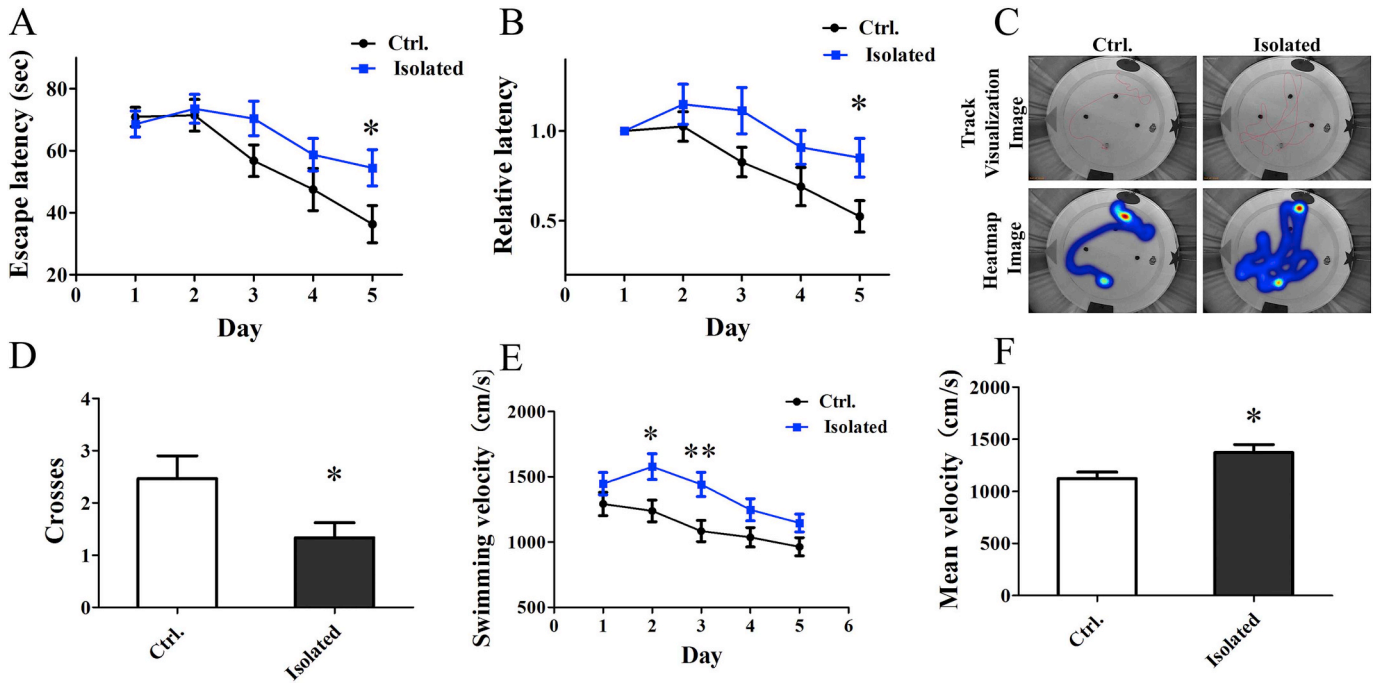

Fig. 3. L-PWSI caused learning and memory deficits in the Balb/c mice in the MWM. (A-E) Acquisition of spatial learning in the different groups of mice after six months of isolation or group housing in the MWM with the hidden platform. **(A)** The escape latencies measured for the isolated and control groups of mice. (B) The relative escape latencies calculated for the isolated and control groups of mice. The escape latencies of the two groups of mice on the first day were normalized to 1.0. The relative escape latencies on the subsequent days were calculated to those on the first day. (C) Representative images of the track visualization path and the heatmap path that the mice swam to find the platform. (D) The number of times that the two groups of mice swam across the target sites after retrieval of the platform. (E) The swimming speed of the two groups of mice on each tested day. (F) The mean swimming speed calculated for the two groups of mice. Data are presented as the mean ± SEM from 22 mice in each group. * represents $p < 0.05$; ** represents $p < 0.01$.

3. Results

3.1. L-PWSI impaired the spatial learning memory of the Balb/c mice

The L-PWSI model mice, which were separated into individual cages from the first weaning day and isolated for 25 weeks, exhibited hyperactive behaviour and aggressive behaviour (greater distance travelled (Fig. 2A, $p < 0.05$) and a longer mobile cumulative duration (Fig. 2B, $p < 0.01$) in the open-field test, but no significance in the mobile velocity, frequency and time in the center area (Fig. 2C-E); longer duration of attack in the social interaction test (Fig. 2F, $p < 0.01$); less inactive cumulative durations in the forced swimming test (Fig. 2G, $p < 0.01$) and tail suspension test (Fig. 2H, $p < 0.01$). These results are consistent with results from recent studies (Rodríguez-Arias et al., 2015; Kumari et al., 2016).

To investigate the navigational ability, spatial learning and memory of the L-PWSI model mice, we performed the MWM experiments. The escape latency to a submerged platform and the number of crossings over the removed platform were compared between the groups (Fig. 3A–D). The L-PWSI mice exhibited impaired learning in the task of locating the submerged escape platform, which was indicated by the increased escape latencies during the trials on the 5th day compared to the escape latencies of the control mice, and the repeated-measures ANOVA also demonstrated a significant difference within-subjects effects (time × group) [$F_{(4, 120)} = 2.532$, $p = 0.044$] (Fig. 3A). We noted that the L-PWSI mice exhibited enhanced swimming speed (Fig. 3F, $p < 0.05$), the repeated-measures ANOVA demonstrated a significant difference between-subjects effects (for group) [$F_{(1, 30)} = 14.187$, $p < 0.001$]; no significant difference within-subjects effects (time × group) [$F_{(3.589, 107.683)} = 0.731$, $p = 0.559$] (Fig. 3E), which highlights the poor performance of the L-PWSI mice. To analyse the results objectively, we normalized the escape latencies from the first trial day of the two groups of the mice to 1.0 and quantified the relative escape latencies from the following trial days relative to those from the first trial day. As shown in Fig. 3B, compared with the control mice that showed intact learning capabilities as indicated by the decreasing relative escape latencies over the training days, the L-PWSI mice showed a lower learning ability, the repeated-measures ANOVA demonstrated a significant difference within-subjects effects (time × group) [$F_{(3.447, 103.442)} = 4.076$, $p = 0.006$].

The swimming speed can strongly affect the outcome (escape latencies and distance swum) of the MWM experiments (Klapdor and van der Staay, 1996), and the inaccurate measure of escape latencies are as a result of the changes in swimming speed. Considering that the measure of the escape latency can be severely biased by strain differences in swimming speed, hence the relative escape latencies are calculated to eliminate the interference of swimming speed. In our search, the isolated mice showed higher velocities in the MWM, which could increase the chances of finding the swimming platform as well as decrease the escape latencies. However, the L-PWSI mice showed increased escape latencies, indicating the poor performance of the L-PWSI mice which is consistent with the increased relative escape latencies. Moreover, the increased swimming speed was exactly in line with the hyperactive behaviour and aggressive behaviour, which corroborated the greater distance travelled and the longer mobile cumulative duration in the open-field test.

In the memory consolidation test, the L-PWSI mice exhibited impaired memory retention; specifically, the L-PWSI mice swam across the target site fewer times than the control mice (Fig. 3D, $p < 0.05$). The results demonstrated that L-PWSI perturbs learning and memory in the Balb/c mice.

3.2. L-PWSI impaired the synaptic plasticity, but synaptic transmission functions were unaffected

LTP has all the hallmarks expected for the cellular processes

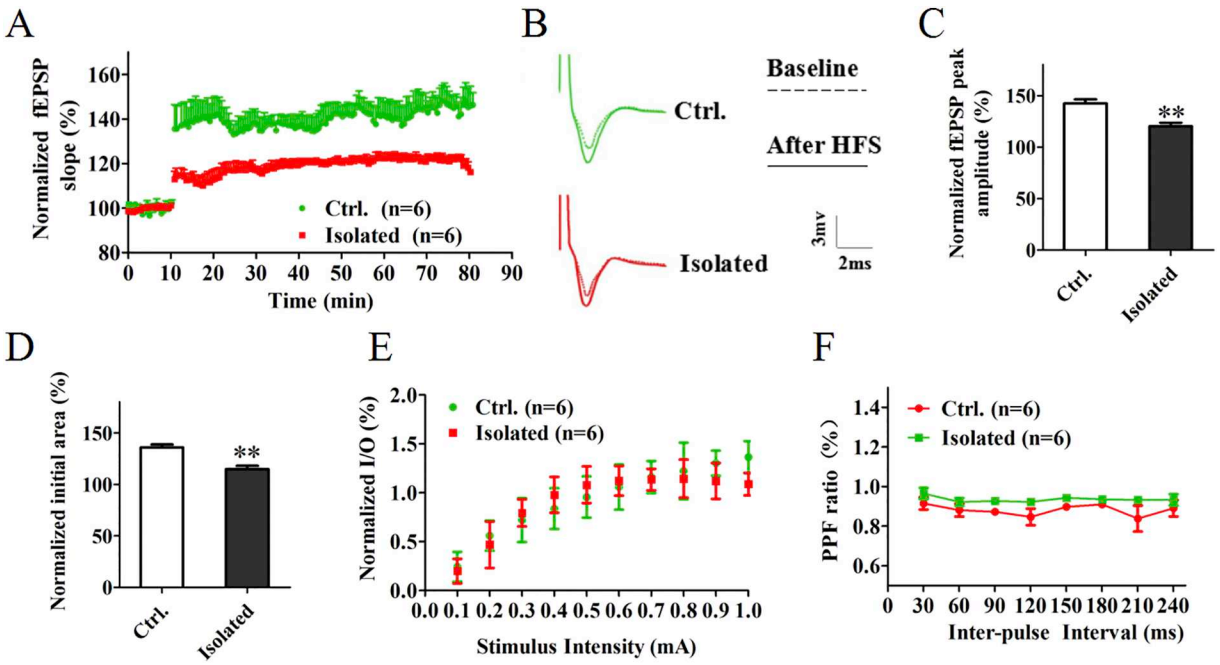

Fig. 4. L-PWSI impaired the synaptic plasticity, but synaptic transmission functions were unaffected. (A) Time course of the effects of high-frequency stimulation (HFS) on the field excitatory postsynaptic potential (fEPSP) initial slope, arrow indicates time when HFS train was applied, and representative fEPSP traces for data in the L-PWSI and control groups. (B) Representative fEPSP traces for data shown in (A). (C) Cumulative data showing the mean fEPSP peak amplitude 70 min post-HFS. (D) Cumulative data showing the mean initial area 70 min post-HFS. (E) The I/O curve of L-PWSI and control groups. (F) The PPF ratio of L-PWSI and control groups. Data are presented as the mean ± SEM from 6 mice in each group. ** represents $p < 0.01$.

underlying learning and memory (Nicoll, 2017), and the mechanisms involved in its generation are essentially the same as those that underlie the synaptic basis of memory (Bliss et al., 2014). Thus, we investigated whether the L-PWSI would affect the synaptic plasticity by recording the LTP. LTP was induced by high-frequency stimulation (four 100 Hz and 1 s trains were delivered 20 s apart) in the CA1 region of 7-month-old Balb/c mice that had been isolated for 25 weeks from the age of postnatal day 21. The results revealed that the L-PWSI mice showed a lower LTP as indicated by a reduction in fEPSP slope (Fig. 4A), fEPSP peak amplitude (Fig. 4C, $p < 0.01$), and initial areas (Fig. 4D, $p < 0.01$) compared with control mice. Generally, much of the focus in the LTP field is concerned with the first hour, and it is now accepted that during the first hour LTP is expressed postsynaptically (Nicoll, 2017). Thus, the lower LTP in the first hour in the L-PWSI mice indicated the long-term social isolation may impair the postsynaptic function and therefore results in the damage of the postsynaptic plasticity.

To test whether the long-term social isolation could affect basic synaptic transmission, we measured the input/output (I/O) functions. The results showed that there was no significant difference between the L-PWSI and control group in the I/O curve within-subjects effects (time × group) [$F_{(4.232,\ 42.319)} = 0.334$, $p = 0.863$] (Fig. 4E), suggesting that the long-term social isolation did not affect the basic synaptic transmission. Herein, our results also showed that the long-term social isolation did not affect the paired pulse facilitation (PPF) within-subjects effects (time × group) [$F_{(7,\ 70)} = 0.325$, $p = 0.940$] (Fig. 4F), a short-term synaptic plasticity depending on changes in transmitter release (Katz and Miledi, 1968), suggesting that basal transmitter release probability may be normal in the L-PWSI mice. These results indicate that the impaired cognition in the L-PWSI mice may be partially induced by the postsynaptic and not presynaptic dysfunction.

3.3. L-PWSI did not affect the glutamate level in the hippocampus of the Balb/c mice

There is a popular belief that glutamate is an incredibly important excitatory neurotransmitter in the mammalian brain, but excess glutamate can cause "excitotoxicity" and result in neuronal death in some diseases and injuries (Bai et al., 2016). In our study, we examined the effect of L-PWSI on hippocampal glutamate release. The results showed the L-PWSI did not significantly change the dialysate concentration of glutamate in the hippocampus, the repeated-measures ANOVA showed no significance between-subjects effects (for group) [$F_{(1,\ 8)} = 0.448$, $p = 0.522$]; within-subjects effects (time × group) [$F_{(3,\ 30)} = 1.042$, $p = 0.392$] (Fig. 5A). Compared with the control mice, the L-PWSI mice did not show significant changes in the extracellular levels of glutamate in the hippocampus (Fig. 5B), which basically corroborated the PPF results, as both highlighted the normal functioning of the presynaptic membrane.

3.4. L-PWSI decreased the protein levels of both the AMPAR and NMDAR glutamate receptors in the hippocampus of the Balb/c mice, but no significance in the mRNA expressions

Plastic change often results from an alteration in the number of neurotransmitter receptors located on a synapse, such as the glutamate receptors AMPAR and NMDAR (NR1, NR2). The results of western-blot showed decreased protein levels of GluA1 in the hippocampus of L-PWSI mice (Fig. 5C.D, $p < 0.01$). Memory loss that occurs as a consequence of ageing is paralleled by the down-regulation of the AMPARs that mediate fast excitatory synaptic transmission (Radin et al., 2016). The NMDARs are implicated in various learning models (Mukherjee and Yuan, 2016), and the decrease in the levels of hippocampal NR1 and NR2B may be associated with the deficits in the spatial learning and memory abilities seen in the L-PWSI mice (Fig. 5C-D). The results of IHC staining further confirmed the decreased protein levels of GluA1 (Fig. 5G.H, $p < 0.05$), NR2B (Fig. 5I.J, $p < 0.05$) and NR1(Fig. 5K.J, $p < 0.05$) in the L-PWSI mice. However, compared with the control mice, L-PWSI mice did not exhibit significant changes in the protein expression of NR2A and $GABA_A$ (Fig. 5C. D). Meanwhile, the results of RT-PCR also showed no significance in the mRNA levels of GluA1, NR1 and NR2B between the control and L-PWSI group (Fig. 5E.F),

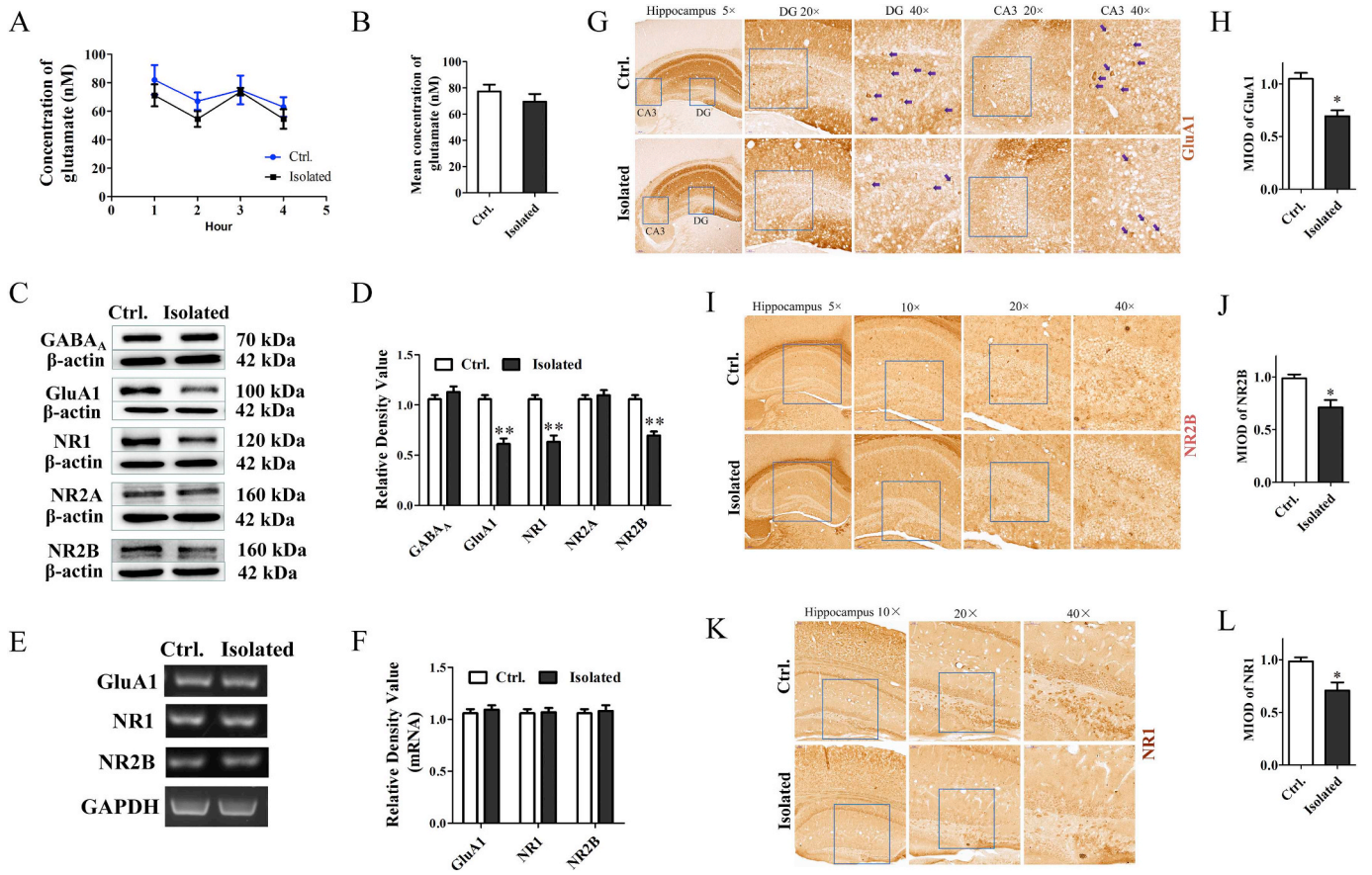

Fig. 5. L-PWSI decreased the protein levels of both the AMPAR and NMDAR glutamate receptors, but the mRNA levels and glutamate release was unaffected. (A) The dialysate concentration of glutamate in the hippocampus of the L-PWSI and control mice. (B) The mean concentration of extracellular glutamate in the hippocampus of the L-PWSI and control mice. Data are presented as the mean ± SEM of 5 mice in each group. (C.D) Representative micrographs of Western bolt and densitometry analysis of $GABA_A$, GluA1, NR1, NR2A and NR2B in the hippocampus of the L-PWSI and control mice. Each data column represents the mean ± SEM obtained from 6 brain samples. (E.F) Representative micrographs of RT-PCR and densitometry analysis of GluA1, NR1 and NR2B in the hippocampus of the L-PWSI and control mice. Each data column represents the mean ± SEM obtained from 3 brain samples. (G-L) The coronal sections of the hippocampus were immunohistochemically stained with an antibody against GluA1, NR2B and NR1, the mean integrated optical density (MIOD) were quantified. Data are presented as the mean ± SEM of 3 mice in each group. * represents $p < 0.05$; ** represents $p < 0.01$.

suggesting the decreased expression level of these proteins were not induced by synthesis deficiency.

3.5. L-PWSI decreased the protein level of PSD-95, but did not affect the presynaptic protein expression in the hippocampus of the Balb/c mice

Synaptophysin is commonly used as an estimate of the number of functional synapses (Tarsa and Goda, 2002). Synapsin I controls the fraction of synaptic vesicles available for release and thereby regulates the efficiency of neurotransmitter release by changing its phosphorylation state (Wu et al., 2016). Both are separated in the presynaptic membrane. Meanwhile, growth associated protein 43 (GAP-43), another presynaptic protein, is enriched in nerve growth cones (Donovan et al., 2002). Using western blot, we measured the protein level of synaptophysin, synapsin I and GAP-43. Compared with the control mice, the L-PWSI mice did not show significant changes in the expression of synaptophysin, synapsin I and GAP-43 in the hippocampus (Fig. 6A. B), which further support the normal activity of the presynaptic membrane.

PSD-95 is one of the most abundant proteins found in the postsynaptic density and plays an important functional role in regulating synaptic transmission and plasticity. Using western blot (Fig. 6A.B, $p < 0.01$), immunofluorescence (Fig. 6F.G, $p < 0.05$) and immunohistochemistry (Fig. 6D.E, $p < 0.01$), we measured the protein level of PSD-95, the results showed that the L-PWSI down-regulated the expression of PSD-95 in the hippocampus (Fig. 5) However, the results of RT-PCR showed no significant change in the mRNA expression level of PSD-95 (Fig. 6C). PSD-95 is distributed in the postsynaptic density of excitatory glutamatergic synapses, interacting with the regulatory subunits of AMPAR and NMDARs targeting, and these associated signaling proteins participate in the information storage process (Gardoni et al., 2001). The enhancement of PSD-95 regulates the strength of synaptic activity, however the decreased protein level of PSD-95 may reduce the development of synaptic structures (Ehrlich et al., 2007), impaired the synaptic activity and memory formation in the L-PWSI mice. Nonetheless, the decreased PSD-95 is a not a surprising result as it echoes the harmony with the lower LTP and support the postsynaptic function theory.

3.6. Rapamycin rescued the deficient autophagy in the hippocampus induced by the L-PWSI and improved cognition function

To explore the possible relationship between autophagic flux and the post-synaptic damage caused by the L-PWSI, we detected the level of autophagy-related proteins. The results showed that the L-PWSI increased the protein expression levels of p-AKT/AKT, p-mTOR/mTOR and p62, decreased the protein expression levels of LC3B and Beclin1 (Fig. 7A-D, $p < 0.01$). Related researches have proved that the activation of PI3K-AKT-mTOR inhibits the autophagy level (Xuan et al., 2017). This then imply that the increased p-AKT/AKT and p-mTOR/mTOR may inhibit the autophagy activity in the L-PWSI mice. LC3B is

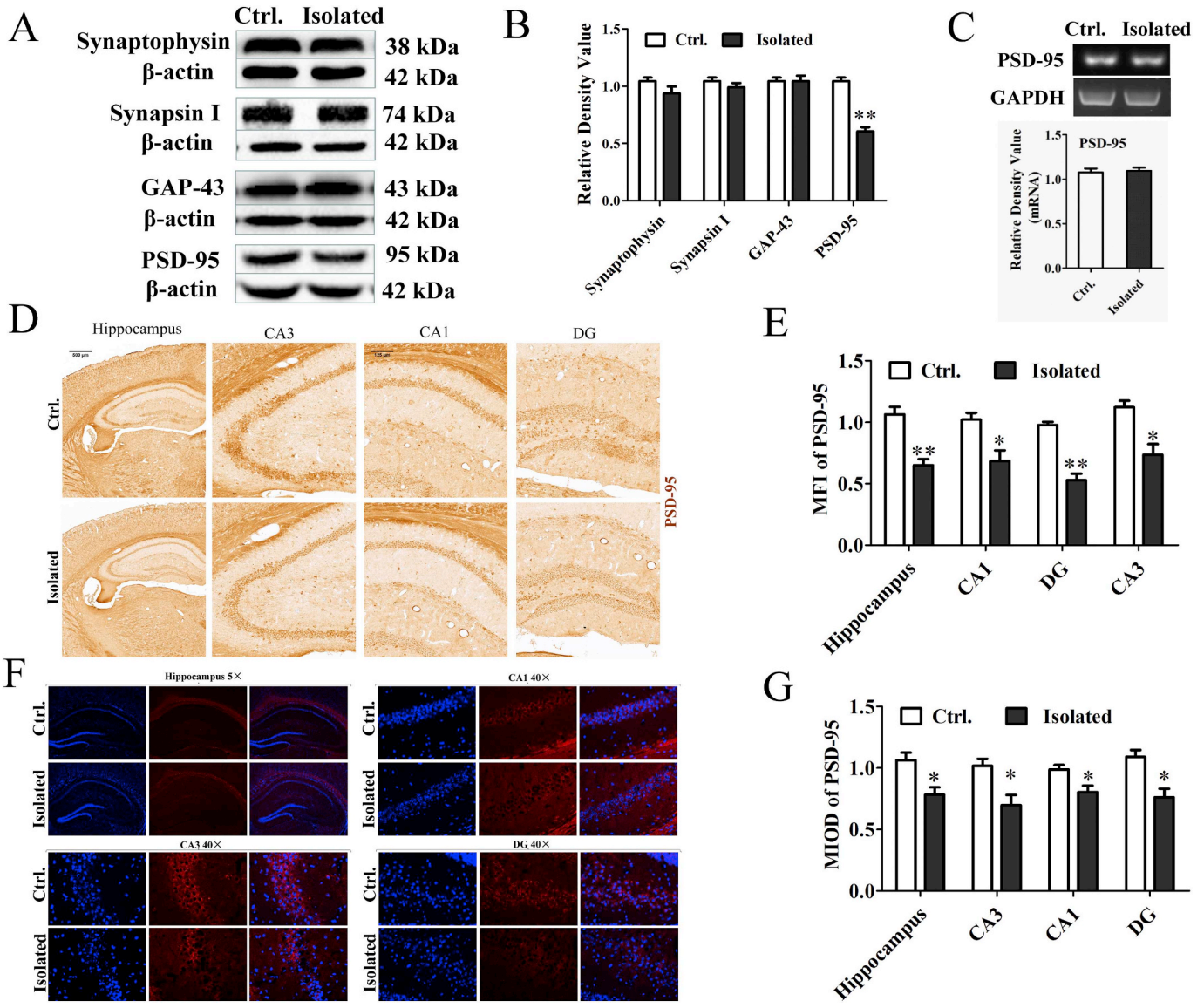

Fig. 6. L-PWSI decreased the protein level of PSD-95, but did not affect the presynaptic protein expression in the hippocampus of the Balb/c mice. (A.B) Representative micrographs of Western blot and densitometry analysis of synaptophysin, synapsin I, GAP-43 and PSD-95 in the hippocampus of the L-PWSI and control mice. Each data column represents the mean ± SEM. obtained from 6 brain samples. (C) Representative micrographs of RT-PCR and densitometry analysis of PSD-95 in the hippocampus of the L-PWSI and control mice. Each data column represents the mean ± SEM. obtained from 3 brain samples. (D) The coronal sections of the hippocampus were immunofluorescent stained with an antibody against PSD-95 (Blue: DAPI; Red: PSD-95). (E) The mean fluorescent intensity (MFI) of PSD-95 immunoreactivity was quantified. (F.G) The coronal sections of the hippocampus were immunohistochemically stained with an antibody against PSD-95, the MIOD for PSD-95 were quantified. Data represent mean ± SEM from 3 mice per group. * represents $p < 0.05$; ** represents $p < 0.01$. (For interpretation of the references to colour in this figure legend, the reader is referred to the web version of this article.)

the most widely used marker to monitor autophagy, and the LC3B-II is a recognized autophagosome marker (Klionsky et al., 2012; Kabeya et al., 2000). The p62, also known as sequestosome1 (SQSTM1), is one of the best-studied autophagy receptors, which is constantly degraded via autophagy and the inhibition of autophagy leads to the accumulation of p62 positive aggregates (Komatsu and Ichimura, 2010). In the present research, the decreased LC3B (LC3B-II) expression marked the deficient autophagy in the L-PWSI mice, and the increase of p62 expression level supported this conclusion from another point. Meanwhile, knock-down of Beclin1 by small interfering RNA (siRNA) inhibited autophagy (Chen et al., 2017b) and the decrease of Beclin1 further indicated a decreased autophagy level induced by L-PWSI.

Researches show that, the upregulation of autophagy by giving rapamycin improves cognitive flexibility and impede the impairments of cognition induced by melamine (Wang et al., 2015; Fu et al., 2017). Herein, the subdued autophagy level may damage the cognitive flexibility, and lost the protective effect to impairments of cognition induced by the L-PWSI. Rapamycin is one of the mTOR inhibitors, two weeks administration of rapamycin did not affect total mTOR targets, while phosphorylated mTOR targets (p-mTOR-Ser2448 and p-AKT-S473) were decreased and LC3-II were increased in cecal ligation and puncture mice (Liu et al., 2017). In our research, intraperitoneal administration of rapamycin (3 mg/kg, i.p.) for 15 days, significantly potentiated the fEPSP slope and peak amplitude [$F_{(3,\ 8)} = 11.46$, $p < 0.01$] (Fig. 7E-G), decreased the protein levels of p-mTOR [$F_{(3,\ 8)} = 45.12$, $p < 0.01$], increased the protein levels of PSD-95 [$F_{(3,\ 8)} = 10.64$, $p < 0.01$], GluA1 [$F_{(3,\ 8)} = 7.369$, $p < 0.05$], NR2B [$F_{(3,\ 8)} = 5.729$, $p < 0.05$] and NR1 [$F_{(3,\ 8)} = 12.89$, $p < 0.01$] (Fig. 7H.I) in the L-PWSI mice. These results suggested rapamycin improves cognition function through enhancing autophagy and may be a potentially

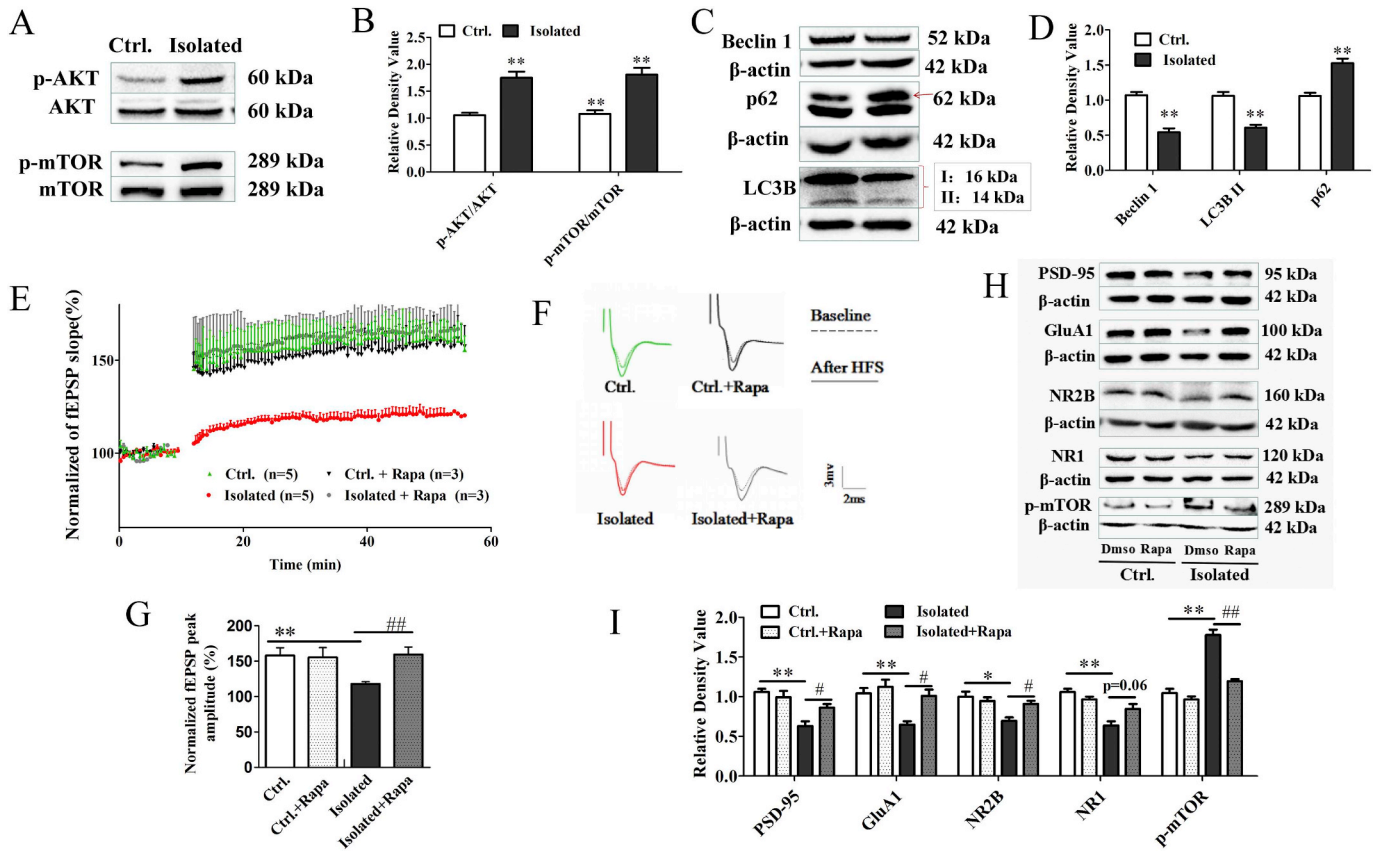

Fig. 7. Deficient autophagy in the hippocampus induced by the L-PWSI. (A-D) Representative micrographs of Western blot and densitometry analysis of p-AKT, AKT, p-mTOR, mTOR, Beclin1, LC3B and p62 in the hippocampus of the L-PWSI and control mice. Each data column represents the mean ± SEM obtained from 6 brain samples. (E-I) Rapamycin reversed the decrease of LTP and cognition-related protein levels induced by the L-PWSI. (E) Time course of the effects of high-frequency stimulation (HFS) on the field excitatory postsynaptic potential (fEPSP) initial slope, arrow indicates time when HFS train was applied, and representative fEPSP traces for data in each group. (F) Representative fEPSP traces for data shown in (E). (G) Cumulative data showing the mean fEPSP peak amplitude 70 min post-HFS. Data are presented as the mean ± SEM from 3 mice in each group. (H–I) Representative micrographs of Western blot and densitometry analysis of PSD-95, GluA1, NR2B, NR1, p-mTOR in the hippocampus after intraperitoneal application of rapamycin. Each data column represents the mean ± SEM obtained from 3 brain samples. *$p < 0.05$, **$p < 0.01$ vs. the control mice; #$p < 0.05$, ##$p < 0.01$ vs. before rapamycin administration in the L-PWSI group.

effective therapeutic agent for the treatment of long-term social isolation-induced cognitive impairment, also implies this causal relationship between the decreased expression levels of cognition-related proteins and the repressed extent of autophagy activation in L-PWSI mice.

4. Discussion

Social isolation can induce anxiety like behavior, recognition memory deficits, conditioned fear memory deficits and object location memory deficits (Green and McCormick, 2013; McIntosh et al., 2013; Okada et al., 2014b); however, the reported effects of social isolation on spatial memory are inconsistent. In this study, we observed that spatial learning and memory, as measured by the MWM, were reduced in the Balb/c mice subjected to L-PWSI. Our data showed that the escape latencies were reduced with the increasing days of training in both groups, which indicated that each group of mice gradually mastered the ability to effectively search for the platform. However, the escape latency and the relative escape latency of the isolated mice were significantly greater than those of the group-housed mice on the 5th day, which demonstrated the learning deficits in the isolated mice. Meanwhile, the isolated mice crossed the platform site significantly fewer times than the group-housed mice on the last day, which further indicated the memory deficit in the isolated mice. All of these results demonstrated the deficiency in spatial memory formation in the L-PWSI mice. Herein, the L-PWSI also exhibited anxiety behaviour and aggressive behaviour which were consistent with results from recent studies (Rodríguez-Arias et al., 2015; Kumari et al., 2016).

Synaptic dysfunction is a strong correlation of cognitive deficits and synaptic plasticity impairments. LTP, as a measurement indicator of synaptic plasticity, is an activity-dependent increase in synaptic efficacy that has all the hallmarks expected for the cellular processes underlying learning and memory (Nicoll, 2017). Thus, we recorded key features of LTP, and found the L-PWSI impaired the first hour LTP, which is expressed postsynaptically (Nicoll, 2017), indicating the deficits in synaptic plasticity of L-PWSI mice may be induced by postsynaptic dysfunction. Meanwhile, the results showed that there was no significant difference between the L-PWSI and control group in the I/O curve and PPF, suggesting that the L-PWSI did not affect the basic synaptic transmission and basal transmitter release probability. This suggests the potential correlation between the cognitive impairment and postsynaptic dysfunction from another perspective.

The synaptic transmission that underlies learning and memory formation requires the combined activity between the presynaptic proteins as well as interaction between the presynaptic proteins and the postsynaptic density proteins (Gąssowska et al., 2016). Our results showed that the L-PWSI did not significantly change the presynaptic synaptophysin, synapsin I and GAP-43 proteins levels. Both synaptophysin and synapsin I are abundant synaptic vesicle proteins which provide the anatomical basis of quantal release of glutamate, and changes in the efficiency of glutamate release are believed to play a major role in synaptic plasticity (Greengard et al., 1993). However, our microdialysis results demonstrated that the L-PWSI did not significantly change the

extracellular level of hippocampal glutamate. The lack of change in the presynaptic protein and glutamate release which verified the above results (no significant changes in the I/O curve and PPF), indicating the normal function on the presynaptic side in the hippocampus of the L-PWSI mice. Interestingly, the L-PWSI decreased the protein expression of postsynaptic PSD-95 in the hippocampus, which is inconsistent with the upregulation of the mRNA expression of PSD-95 in the hippocampus of rats isolated for 8 weeks (Zhao et al., 2009). Increased levels of synaptic PSD-95 is believed to recruit new AMPA receptors to the synapse and depletion of PSD-95 can result in hippocampal neuronal cell death (Gomperts and Donfield, 1996; Gardoni et al., 2001). In this study, the decreased level of hippocampal PSD-95 may disrupt the normal function of the hippocampal neurons in the L-PWSI mice and cause deficits in learning and cognitive function, which further indicated that the L-PWSI damaged cognitive function through the postsynaptic proteins not presynaptic proteins.

The induction and early expression mechanisms of LTP depend on activation and rapid modulation of ionotropic glutamate receptors, including AMPAR and NMDARs, and PSD-95 plays a critical role in postsynaptic AMPAR targeting. Ca^{2+} influx through NMDARs can cause PSD-95 to be temporarily released from postsynaptic membranes (Schnell et al., 2002), and this release seems to represent an important step for postsynaptic restructuring. One pilot microarray study found that AMPARs were upregulated in the prefrontal cortex of isolation-reared rats (Levine et al., 2007). However, our results showed that the level of GluA1 was decreased in the hippocampus of the L-PWSI mice, which echoed the decrease seen in PSD-95. Indeed, stimulation of AMPARs causes the activation of NMDARs and thereby increases the intracellular Ca^{2+}/Na^{+} level (Sturgill et al., 2009). In our study, L-PWSI decreased hippocampal GluA1 protein levels, which may reduce Ca^{2+} influx through NMDARs and cause a further decrease in the PSD-95 protein levels.

We examined the expression of the NR1 subunits because all the NMDARs require at least one of these proteins for channel activity (Meguro et al., 1992; Okada et al., 2014a). Given the available evidence, it was predicted that heterozygous NR1 (+/−) mice with impairment of glutamate function would be more sensitive to the detrimental effects of social isolation (Featherstone et al., 2015). This discovery perfectly complements the confirmation of the decrease in NR1 in the isolated mice in our study, which was also in accordance with Okada's result (Okada et al., 2014a). The results also showed that the hippocampal level of NR2B decreased in the L-PWSI mice, but the hippocampal level of NR2A and $GABA_A$ in the L-PWSI mice did not significantly change compared to that in the control mice. It must be noted however that Xiaohong Zhao et al., found that the mRNA expression levels of NR2A and NR2B were significantly up-regulated in the hippocampus of rats isolated for 8 weeks (Zhao et al., 2009). According to recent evidence, we know that decreased glutamatergic activity may result in several of the core features of schizophrenia (Featherstone et al., 2015), which can be reproduced by administering NMDA antagonists to healthy subjects. The decreased NR2B in the L-PWSI mice seems to confirm this discovery to a certain extent. From another point of view, NR2B plays a critical role in determining the direction of postsynaptic changes (Lanté et al., 2006), and the decrease in NR2B and postsynaptic PSD-95 seem to reflect the dysfunction of the postsynaptic neurons in the L-PWSI mice. The decrease in PSD-95, GluA1, NR1 and NR2B induced postsynaptic dysfunction and greatly damaged synaptic plasticity, partially mediated the deficits observed in memory formation and cognition in the L-PWSI mice.

The role of autophagy in synaptic plasticity is indeed fascinating, the basal autophagy positively regulates synapse development (Shen and Ganetzky, 2009). Researches have also reported that the local presynaptic autophagy degrades synaptic vesicles and rapidly inhibits neurotransmitter release (Sanchez-Varo et al., 2012). NMDARs-dependent autophagy has been shown to induce AMPAR degradation through PI3K-Akt-mTOR pathway (Shehata et al., 2013). In this present study, the L-PWSI increased the protein expressions of p-AKT/AKT, p-mTOR/mTOR and p62 and decreased the protein levels of LC3B and Beclin1, indicating the decreased autophagy. This decrease in autophagy could mean that autophagic degradation pathway was happening and this could also explain the reason for the decreased levels of AMPAR (GluA1) and NMDAR (NR1/NR2B). The upregulation of autophagy by giving rapamycin improves cognitive flexibility and impede the impairments of cognition induced by melamine (Wang et al., 2015; Fu et al., 2017). Herein, the subdued autophagy level may damage the cognitive flexibility, and cause the loss of protective effect against cognition impairments induced by the L-PWSI. Rapamycin, an mTOR inhibitor, was administered to further confirm the causal relationship between the decreased expression of synaptic-related protein levels and the repressed extent of autophagy activation. Rapamycin improves learning after sepsis through enhancing autophagy (Liu et al., 2017), and also rescues vascular, metabolic and learning deficits in apolipoprotein E4 transgenic mice with pre-symptomatic Alzheimer's disease (Lin et al., 2017b). Our results showed the activation of autophagy significantly reversed the decreased synaptic-related protein levels, and recovered the lower LTP induced by the L-PWSI, which may be a potentially effective therapeutic agent for the treatment of long-term social isolation-induced cognitive impairment. However, weather the administration of rapamycin will improve the learning and memory function in the MWM has not been verified.

Our results indicate that the decrease in AMPAR, NR1 and NR2B induced by L-PWSI may disrupted the excitability of neurons, decreased release of PSD-95 from postsynaptic membranes and later adversely impacts postsynaptic restructuring to further results in the dysfunction of synaptic plasticity. The deficient LTP, PSD-95 and NR2B, as well as the stable I/O, PPF, extracellular glutamate and the presynaptic-protein levels, all these results indicated that the postsynaptic, not presynaptic dysfunction, is responsible for the impaired cognition function in the hippocampus. Meanwhile, the decreased level of autophagy may lead to lose of protective function of neurons against cognition impairment. However, the relationship between postsynaptic dysfunction and deficient autophagy, and their involvement in the mechanisms of cognitive disorders merit future research.

5. Conclusions

These results suggested that the L-PWSI activated the mTOR to inhibit the autophagy system and elicited postsynaptic dysfunction through disruption of the cross interaction between GluA1, NMDARs and PSD-95. Both could potentially lead to impaired synaptic plasticity and damaged spatial memory and cognitive function.

Acknowledgements

This study was supported by the National Natural Science Foundation of China (81571061, 81671061), Natural science foundation of Liaoning province of China (201602218, 2015020672) and Scientific Study Project for Institutes of Higher Learning, Ministry of Education, Liaoning Province (LZ2017001).

Conflict of interest statement

The research was conducted in the absence of any commercial or financial relationships that could be misconstrued as a potential conflict of interest. We confirm that all authors contributed to this manuscript and have approved the final article.

Appendix A. Supplementary data

Supplementary data to this article can be found online at https://doi.org/10.1016/j.expneurol.2018.09.009.

References

Arnett, J.J., 2000. Emerging adulthood. A theory of development from the late teens through the twenties. Am Psychol 55 (5), 469–480. https://doi.org/10.1037/0003-066X.55.5.469.

Avdalyan, A.M., Kobyakov, D.S., Klimachev, V.V., Bobrov, I.P., Lazarev, A.F., Pichigina, A.K., et al., 2015. Expression of B23/Nucleophosphamine Nonribosomal Nucleolar Protein in Smooth Muscle Tumors of the Corpus Uteri. Bull. Exp. Biol. Med. 160 (2), 286–290. https://doi.org/10.1007/s10517-015-3152-x.

Bai, X., Zhang, C., Chen, A., Liu, W., Li, J., Sun, Q., et al., 2016. Protective effect of edaravone on glutamate-induced neurotoxicity in spiral ganglion neurons. Neural Plast 2016, 4034218.

Bliss, T.V., Collingridge, G.L., 1993. A synaptic model of memory: long-term potentiation in the hippocampus. Nature 361, 31–39. https://doi.org/10.1038/361031a0.

Bliss, T.V.P., Collingridge, G.L., Morris, R.G.M., 2014. Synaptic plasticity in health and disease: introduction and overview. Philos. Trans. R. Soc. Lond. Ser. B Biol. Sci. 369, 20130129. https://doi.org/10.1098/rstb.2013.0129.

Brenhouse, H.C., Andersen, S.L., 2011. Developmental trajectories during adolescence in males and females: a cross-species understanding of underlying brain changes. Neurosci. Biobehav. Rev. 35 (8), 1687–1703. https://doi.org/10.1016/j.neubiorev.2011.04.013.

Chen, L.L., Feng, H.F., Mao, X.X., Ye, Q., Zeng, L.H., 2013. One hour of pilocarpine-induced status epilepticus is sufficient to develop chronic epilepsy in mice, and is associated with mossy fiber sprouting but not neuronal death. Neurosci. Bull. 29 (3), 295–302. https://doi.org/10.1007/s12264-013-1310-6.

Chen, W., An, D., Xu, H., Cheng, X., Wang, S., Yu, W., et al., 2017a. Effects of social isolation and re-socialization on cognition and ADAR1 (p110) expression in mice. PeerJ 4, e2306. https://doi.org/10.7717/peerj.2306.

Chen, J., Yu, Y., Li, S., Liu, Y., Zhou, S., Cao, S., et al., 2017b. MicroRNA-30a ameliorates hepatic fibrosis by inhibiting Beclin1-mediated autophagy. J. Cell. Mol. Med. 21 (12), 3679–3692. https://doi.org/10.1111/jcmm.13278.

Cordaro, M., Impellizzeri, D., Paterniti, I., Bruschetta, G., Siracusa, R., De Stefano, D., et al., 2016. Neuroprotective effects of Co-UltraPEALut on secondary inflammatory process and autophagy involved in traumatic brain injury. J. Neurotrauma 33 (1), 132–146. https://doi.org/10.1089/neu.2014.3460.

Cryan, J.F., Mombereau, C., Vassout, A., 2015. The tail suspension test as a model for assessing antidepressant activity: review of pharmacological and genetic studies in mice. Neurosci. Biobehav. Rev. 29 (4–5), 571–625.

Ding, Y., Qiao, A., Wang, Z., Goodwin, J.S., Lee, E.S., Block, M.L., et al., 2008. Retinoic acid attenuates beta-amyloid deposition and rescues memory deficits in an Alzheimer's disease transgenic mouse model. J Neurosci 28 (45), 11622–11634. https://doi.org/10.1523/JNEUROSCI.3153-08.2008.

Donovan, S.L., Mamounas, L.A., Andrews, A.M., Blue, M.E., McCasland, J.S., 2002. GAP-43 is critical for normal development of the serotonergic innervation in forebrain. J. Neurosci. 22 (9), 3543–3552.

Ehrlich, I., Klein, M., Rumpel, S., Malinow, R., 2007. PSD-95 is required for activity-driven synapse stabilization. Proc. Natl. Acad. Sci. U. S. A. 104 (10), 4176–4181.

Featherstone, R.E., Shin, R., Kogan, J.H., Liang, Y., Matsumoto, M., Siegel, S.J., 2015. Mice with subtle reduction of NMDA NR1 receptor subunit expression have a selective decrease in mismatch negativity: implications for schizophrenia prodromal population. Neurobiol. Dis. 73, 289–295. https://doi.org/10.1016/j.nbd.2014.10.010.

Fu, J., Wang, H., Gao, J., Yu, M., Wang, R., Yang, Z., 2017. Rapamycin effectively impedes melamine-induced impairments of cognition and synaptic plasticity in wistar rats. Mol. Neurobiol. 54 (2), 819–832. https://doi.org/10.1007/s12035-016-9687-7.

Gardoni, F., Schrama, L.H., Kamal, A., Gispen, W.H., Cattabeni, F., Di Luca, M., 2001. Hippocampal synaptic plasticity involves competition between Ca2+/calmodulin-dependent protein kinase II and postsynaptic density 95 for binding to the NR2A subunit of the NMDA receptor. J. Neurosci. 21 (5), 1501–1509.

Gąssowska, M., Baranowska-Bosiacka, I., Moczydłowska, J., Frontczak-Baniewicz, M., Gewartowska, M., Strużyńska, L., et al., 2016. Perinatal exposure to lead (Pb) induces ultrastructural and molecular alterations in synapses of rat offspring. Toxicology 2016 (29). https://doi.org/10.1016/j.tox.2016.10.014.

Gomperts, E.D., Donfield, S.M., 1996. Ethics of AIDS study. Science 274 (5293), 1596b.

Green, M.R., McCormick, C.M., 2013. Effects of social instability stress in adolescence on long-term, not short-term, spatial memory performance. Behav. Brain Res. 256, 165–171. https://doi.org/10.1016/j.bbr.2013.08.011.

Greengard, P., Valtorta, F., Czernik, A.J., Benfenati, F., 1993. Synaptic vesicle phosphoproteins and regulation of synaptic function. Science 259 (5096), 780–785.

Hara, T., Nakamura, K., Matsui, M., Yamamoto, A., Nakahara, Y., Suzuki-Migishima, R., et al., 2006. Suppression of basal autophagy in neural cells causes neurodegenerative disease in mice. Nature 441, 885e9. https://doi.org/10.1038/nature04724.

Hellemans, K.G., Benge, L.C., Olmstead, M.C., 2004. Adolescent enrichment partially reverses the social isolation syndrome. Brain Res. Dev. Brain Res. 150 (2), 103–115. https://doi.org/10.1016/j.devbrainres.2004.03.003.

Hsieh, C.H., Pai, P.Y., Hsueh, H.W., Yuan, S.S., Hsieh, Y.C., 2011. Complete induction of autophagy is essential for cardioprotection in sepsis. Ann. Surg. 253, 1190–1200. https://doi.org/10.1097/SLA.0b013e318214b67e.

Jung, T.G., Lee, J.H., Lee, I.S., Choi, B.T., 2010. Involvement of intracellular calcium on the phosphorylation of spinal N-methyl-D-aspartate receptor following electro-acupuncture stimulation in rats. Acta Histochem. 112 (2), 127–132. https://doi.org/10.1016/j.acthis.2008.09.009.

Kabeya, Y., Mizushima, N., Ueno, T., Yamamoto, A., Kirisako, T., Noda, T., et al., 2000. LC3, a mammalian homologue of yeast Apg8p, is localized in autophagosome membranes after processing. EMBO J. 19 (21), 5720–5728. https://doi.org/10.1093/emboj/19.21.5720.

Katz, B., Miledi, R., 1968. The role of calcium in neuromuscular facilitation. J. Physiol. 195, 481–492.

Kaushik, S., Rodriguez-Navarro, J.A., Arias, E., Kiffin, R., Sahu, S., Schwartz, G.J., et al., 2011. Autophagy in hypothalamic AgRP neurons regulates food intake and energy balance. Cell Metab. 14 (2), 173–183. https://doi.org/10.1016/j.cmet.2011.06.008.

Khodaie, B., Lotfinia, A.A., Ahmadi, M., Lotfinia, M., Jafarian, M., Karimzadeh, F., et al., 2015. Structural and functional effects of social isolation on the hippocampus of rats with traumatic brain injury. Behav. Brain Res. 278, 55–65. https://doi.org/10.1016/j.bbr.2014.09.034.

Klapdor, K., van der Staay, F.J., 1996. The Morris water-escape task in mice: strain differences and effects of intra-maze contrast and brightness. Physiol. Behav. 60 (5), 1247–1254. https://doi.org/10.1016/S0031-9384(96)00224-7.

Klionsky, D.J., Abdalla, F.C., Abeliovich, H., Abraham, R.T., Acevedo-Arozena, A., Adeli, K., et al., 2012. Guidelines for the use and interpretation of assays for monitoring autophagy. Autophagy 8, 445–544.

Komatsu, M., Ichimura, Y., 2010. Physiological significance of selective degradation of p62 by autophagy. FEBS Lett. 584, 1374–1378. https://doi.org/10.1016/j.febslet.2010.02.017.

Komatsu, M., Waguri, S., Chiba, T., Murata, S., Iwata, J., Tanida, I., et al., 2006. Loss of autophagy in the central nervous system causes neurodegeneration in mice. Nature 441 (7095), 880e4. https://doi.org/10.1038/nature04723.

Kumari, A., Singh, P., Baghel, M.S., Thakur, M.K., 2016. Social isolation mediated anxiety like behavior is associated with enhanced expression and regulation of BDNF in the female mouse brain. Physiol. Behav. 158, 34–42. https://doi.org/10.1016/j.physbeh.2016.02.032.

Kwon, S.E., Chapman, E.R., 2011. Synaptophysin regulates the kinetics of synaptic vesicle endocytosis in central neurons. Neuron 70 (5), 847–854. https://doi.org/10.1016/j.neuron.2011.04.001.

Lanté, F., de Jésus Ferreira, M.C., Guiramand, J., Récasens, M., Vignes, M., 2006. Low-frequency stimulation induces a new form of LTP, metabotropic glutamate (mGlu5) receptor- and PKA-dependent, in the CA1 area of the rat hippocampus. Hippocampus 16 (4), 345–360. https://doi.org/10.1002/hipo.20146.

Lau, A., Zheng, Y., Tao, S.S., Wang, H.H., Whitman, S.A., White, E., et al., 2013. Arsenic inhibits autophagic flux, activating the Nrf2-Keap1 pathway in a p62-dependent manner. Mol. Cell. Biol. 33 (12), 2436–2446. https://doi.org/10.1128/MCB.01748-12.

Levine, J.B., Youngs, R.M., MacDonald, M.L., Chu, M., Leeder, A.D., Berthiaume, F., et al., 2007. Isolation rearing and hyperlocomotion are associated with reduced immediate early gene expression levels in the medial prefrontal cortex. Neuroscience 145 (1), 42–55. https://doi.org/10.1016/j.neuroscience.2006.11.063.

Lin, X., Han, Y., Li, P., Shi, L., Lu, L., 2017a. Economic "activity-silent" synaptic mechanisms of working memory. Neurosci. Bull. 33 (6), 760–762. https://doi.org/10.1007/s12264-017-0158-6.

Lin, A.L., Jahrling, J.B., Zhang, W., Derosa, N., Bakshi, V., Romero, P., et al., 2017b. Rapamycin rescues vascular, metabolic and learning deficits in apolipoprotein E4 transgenic mice with pre-symptomatic Alzheimer's disease. J. Cereb. Blood Flow Metab. 37 (1), 217–226.

Liu, F., Day, M., Muñiz, L.C., Bitran, D., Arias, R., Revilla-Sanchez, R., et al., 2008. Activation of estrogen receptor-beta regulates hippocampal synaptic plasticity and improves memory. Nat. Neurosci. 11 (3), 334–343. https://doi.org/10.1038/nn2057.

Liu, W., Guo, J., Mu, J., Tian, L., Zhou, D., 2017. Rapamycin protects sepsis-induced cognitive impairment in mouse hippocampus by enhancing autophagy. Cell. Mol. Neurobiol. 37 (7), 1195–1205. https://doi.org/10.1007/s10571-016-0449-x.

Lu, L., Bao, G., Chen, H., Xia, P., Fan, X., Zhang, J., et al., 2003. Modification of hippocampal neurogenesis and neuroplasticity by social environments. Exp. Neurol. 183 (2), 600–609. https://doi.org/10.1016/S0014-4886(03)00248-6.

Ma, J., Wang, F., Yang, J., Dong, Y., Su, G., Zhang, K., et al., 2017. Xiaochaihutang attenuates depressive/anxiety-like behaviors of social isolation-reared mice by regulating monoaminergic system, neurogenesis and BDNF expression. J. Ethnopharmacol. 208, 94–104. https://doi.org/10.1016/j.jep.2017.07.005.

McIntosh, A.L., Ballard, T.M., Steward, L.J., Moran, P.M., Fone, K.C., 2013. The atypical antipsychotic risperidone reverses the recognition memory deficits induced by post-weaning social isolation in rats. Psychopharmacology 228 (1), 31–42. https://doi.org/10.1007/s00213-013-3011-2.

Meguro, H., Mori, H., Araki, K., Kushiya, E., Kutsuwada, T., Yamazaki, M., et al., 1992. Functional-characterization of a heteromeric NMDA receptor channel expressed from cloned cDNAs. Nature 357 (6373), 70–74. https://doi.org/10.1038/357070a0.

Morris, R., 1984. Developments of a water-maze procedure for studying spatial learning in the rat. J. Neurosci. Methods 11 (1), 47–60. https://doi.org/10.1016/0165-0270(84)90007-4.

Mukherjee, B., Yuan, Q., 2016. NMDA receptors in mouse anterior piriform cortex initialize early odor preference learning and L-type calcium channels engage for long-term memory. Sci. Rep. 6, 35256. https://doi.org/10.1038/srep35256.

Murai, T., Okuda, S., Tanaka, T., Ohta, H., 2007. Characteristics of object location memory in mice: behavioral and pharmacological studies. Physiol. Behav. 90 (1), 116–124. https://doi.org/10.1016/j.physbeh.2006.09.013.

Negru-Subtirica, O., Tiganasu, A., Dezutter, J., Luyckx, K., 2016. A cultural take on the links between religiosity, identity, and meaning in life in religious emerging adults. Br J Dev Psychol. https://doi.org/10.1111/bjdp.12169. (Dec 26).

Nicoll, R.A., 2017. A brief history of long-term potentiation. Neuron 93 (2), 281–290. https://doi.org/10.1016/j.neuron.2016.12.015.

Okada, R., Matsumoto, K., Tsushima, R., Fujiwara, H., Tsuneyama, K., 2014a. Social isolation stress-induced fear memory deficit is mediated by down-regulated neurosignaling system and Egr-1 expression in the brain. Neurochem. Res. 39 (5), 875–882. https://doi.org/10.1007/s11064-014-1283-5.

Okada, Ryo, Matsumoto, Kinzo, Tsushima, Ryohei, Fujiwara, Hironori, Tsuneyama,

Koichi, 2014b. Social isolation stress-induced fear memory deficit is mediated by down-regulated neuro-signaling system and Egr-1 expression in the brain. Neurochem. Res. 39 (5), 875–882. https://doi.org/10.1007/s11064-014-1283-5.
O'Keefe, L.M., Doran, S.J., Mwilambwe-Tshilobo, L., Conti, L.H., Venna, V.R., McCullough, L.D., 2014. Social isolation after stroke leads to depressive-like behavior and decreased BDNF levels in mice. Behav. Brain Res. 260, 162–170. https://doi.org/10.1016/j.bbr.2013.10.047.
Paus, T., Keshavan, M., Giedd, J.N., 2008. Why do many psychiatric disorders emerge during adolescence? Nat. Rev. Neurosci. 9 (12), 947–957. https://doi.org/10.1038/nrn2513.
Poels, J., Spasic, M.R., Callaerts, P., Norga, K.K., 2012. An appetite for destruction: from self-eating to cell cannibalism as a neuronal survival strategy. Autophagy 8 (9), 1401–1403. https://doi.org/10.4161/auto.21052.
Radin, D.P., Zhong, S., Purcell, R., Lippa, A., 2016. Acute ampakine treatment ameliorates age-related deficits in long-term potentiation. Biomed Pharmacother 84, 806–809. https://doi.org/10.1016/j.biopha.2016.10.016.
Riley, J.L., Noble, D.W., Byrne, R.W., Whiting, M.J., 2016. Does social environment influence learning ability in a family-living lizard? Anim Cogn. https://doi.org/10.1007/s10071-016-1068-0. (Dec 26).
Rodríguez-Arias, M., Navarrete, F., Blanco-Gandia, M.C., Arenas, M.C., Aguilar, M.A., Bartoll-Andrés, A., et al., 2015. Role of CB2 receptors in social and aggressive behavior in male mice. Psychopharmacology 232 (16), 3019–3031. https://doi.org/10.1007/s00213-015-3939-5.
Sanchez-Varo, R., Trujillo-Estrada, L., Sanchez-Mejias, E., Torres, M., Baglietto-Vargas, D., Moreno-Gonzalez, I., et al., 2012. Abnormal accumulation of autophagic vesicles correlates with axonal and synaptic pathology in young Alzheimer's mice hippocampus. Acta Neuropathol. 123 (1), 53–70. https://doi.org/10.1007/s00401-011-0896-x.
Schnell, E., Sizemore, M., Karimzadegan, S., Chen, L., Bredt, D.S., Nicoll, R.A., 2002. Direct interactions between PSD-95 and stargazin control synaptic AMPA receptor number. Proc. Natl. Acad. Sci. U. S. A. 99 (21), 13902–13907. https://doi.org/10.1073/pnas.172511199.
Shehata, M., Matsumura, H., Okubo-Suzuki, R., Ohkawa, N., Inokuchi, K., 2013. Neuronal stimulation induces autophagy in hippocampal neurons that is involved in AMPA receptor degradation after chemical long-term depression. J. Neurosci. 32 (30), 10413–10422. https://doi.org/10.1523/JNEUROSCI.4533-11.2012.
Shen, W., Ganetzky, B., 2009. Autophagy promotes synapse development in Drosophila. J. Cell Biol. 187 (1), 71–79. https://doi.org/10.1083/jcb.200907109.
Sturgill, J.F., Steiner, P., Czervionke, B.L., Sabatini, B.L., 2009. Distinct domains within PSD-95 mediate synaptic incorporation, stabilization, and activity-dependent trafficking. J. Neurosci. 29 (41), 12845–12854. https://doi.org/10.1523/JNEUROSCI.1841-09.2009.
Tao, K., Wang, B., Feng, D., Zhang, W., Lu, F., Lai, J., et al., 2016. Salidroside protects against 6-hydroxydopamine-induced cytotoxicity by attenuating ER stress. Neurosci. Bull. 32 (1), 61–69. https://doi.org/10.1007/s12264-015-0001-x.
Tarsa, L., Goda, Y., 2002. Synaptophysin regulates activity-dependent synapse formation in cultured hippocampal neurons. Proc. Natl. Acad. Sci. U. S. A. 99 (2), 1012–1016. https://doi.org/10.1073/pnas.022575999.
Volianskis, A., France, G., Jensen, M.S., Bortolotto, Z.A., De, Jane, Collingridge, G.L., 2015. Long-term potentiation and the role of N-methyl-D-aspartate receptors. Brain Res. 1621, 5–16. https://doi.org/10.1016/j.brainres.2015.01.016.
Wang, Hui, Peng, Rui-Yun, 2016. Basic roles of key molecules connected with NMDAR signaling pathway on regulating learning and memory and synaptic plasticity. Mil Med Res 3 (1), 26. https://doi.org/10.1186/s40779-016-0095-0.
Wang, H., Gao, N., Li, Z., Yang, Z., Zhang, T., 2015. Autophagy alleviates melamine-induced cell death in PC12 cells via decreasing ROS level. Mol. Neurobiol. https://doi.org/10.1007/s12035-014-9073-2.
Wang, J., Lu, W., Chen, L., Zhang, P., Qian, T., Cao, W., et al., 2016. Serine 707 of APPL1 is critical for the synaptic NMDA receptor-mediated Akt phosphorylation signaling pathway. Neurosci. Bull. 32 (4), 323–330. https://doi.org/10.1007/s12264-016-0042-9.
Wang, B., Wang, Y., Wu, Q., Huang, H.P., Li, S., 2017. Effects of α2A adrenoceptors on norepinephrine secretion from the locus coeruleus during chronic stress-induced depression. Front. Neurosci. 11, 243. https://doi.org/10.3389/fnins.2017.00243.
Wongwitdecha, N., Marsden, C.A., 1996. Effects of social isolation rearing on learning in the Morris water maze. Brain Res. 715 (1–2), 119–124. https://doi.org/10.1016/0006-8993(95)01578-7.
Wu, J., Chen, H., Li, H., Tang, Y., Yang, L., Cao, S., et al., 2016. Antidepressant potential of chlorogenic acid-Enriched extract from eucommia ulmoides oliver bark with neuron protection and promotion of serotonin release through enhancing synapsin I expression. Molecules 21 (3), 260. https://doi.org/10.3390/molecules21030260.
Xuan, F., Jian, J., Lin, X., Huang, J., Jiao, Y., Huang, W., et al., 2017. 17-methoxyl-7-hydroxybenzene-furanchalcone ameliorates myocardial ischemia/reperfusion injury in rat by inhibiting apoptosis and autophagy via the PI3K-Akt signal pathway. Cardiovasc. Toxicol. 301, 79–87. https://doi.org/10.1007/s12012-016-9358-y.
Yen, Y.T., Yang, H.R., Lo, H.C., Hsieh, Y.C., Tsai, S.C., Hong, C.W., et al., 2013. Enhancing autophagy with activated protein C and rapamycin protects against sepsis-induced acute lung injury. Surgery 153, 689–698. https://doi.org/10.1016/j.surg.2012.11.021.
Yusufishaq, S., Rosenkranz, J.A., 2013. Post-weaning social isolation impairs observational fear conditioning. Behavioual Brain Research 1 (242), 142–149. https://doi.org/10.1016/j.bbr.2012.12.050.
Zaidan, H., Gaisler-Salomon, I., 2015. Prereproductive stress in adolescent female rats affects behavior and corticosterone levels in second-generation offspring. Psychoneuroendocrinology 58, 120–129. https://doi.org/10.1016/j.psyneuen.2015.04.013.
Zhang, M.Y., Zheng, C.Y., Zou, M.M., Zhu, J.W., Zhang, Y., Wang, J., et al., 2014. Lamotrigine attenuates deficits in synaptic plasticity and accumulation of amyloid plaques in APP/PS1 transgenic mice. Neurobiol. Aging 35 (12), 2713–2725. https://doi.org/10.1016/j.neurobiolaging.2014.06.009.
Zhao, X., Sun, L., Jia, H., Meng, Q., Wu, S., Li, N., et al., 2009. Isolation rearing induces social and emotional function abnormalities and alters glutamate and neurodevelopment-related gene expression in rats. Prog. Neuro-Psychopharmacol. Biol. Psychiatry 33 (7), 1173–1177. https://doi.org/10.1016/j.pnpbp.2009.06.016.